Construction and Building Materials 199 (2019) 1–11

Contents lists available at ScienceDirect

Construction and Building Materials

journal homepage: www.elsevier.com/locate/conbuildmat

Study on dispersion, mechanical and microstructure properties of cement paste incorporating graphene sheets

Jintao Liu [a], Jiali Fu [a], Yang Yang [a,b,*], Chunping Gu [a]

[a] College of Architecture and Civil Engineering, Zhejiang University of Technology, Hangzhou 310014, China
[b] Key Laboratory of Civil Engineering Structures & Disaster Prevention and Mitigation Technology of Zhejiang Province, Hangzhou 310014, China

HIGHLIGHTS

- Dispersion of graphene in water is evaluated with different surfactants.
- Graphene addition in cement paste increase strengths significantly.
- Appropriate amount of graphene improves microstructure of composite.

ARTICLE INFO

Article history:
Received 24 September 2018
Received in revised form 27 November 2018
Accepted 2 December 2018

Keywords:
Graphene
Mechanical properties
Dispersion
Microstructure

ABSTRACT

In this study, the influences of ultrasonic and surfactants on the dispersion of graphene sheets in water were evaluated using UV–vis spectroscopy, and homogenous dispersions of graphene sheets in water were obtained by using sodium dodecyl benzene sulfonate (SDBS). Then, the highly dispersed graphene sheets were introduced to cement paste through high-speed mixing, and the mechanical and microstructural properties of graphene-modified cement material was evaluated. Experiment results indicated that the addition of 0.025 wt% graphene sheets increased the 7-day composite compressive strength by 14.9%, the flexural strength by 23.6% and direct tensile strength by 15.2%. X-ray diffraction (XRD) analysis showed that the addition of graphene sheets lowered the orientation index of calcium hydroxide (CH) crystals significantly. Moreover, mercury intrusion porosimetry (MIP) and microscope imaging (SEM) indicated that a high degree of dispersion of graphene sheets was achieved, and the two-dimensional graphene sheets promote hydration and suppress the extension process of cracks.

1. Introduction

As a main component of concrete, cement is the most widely used binder material in the world. However, one of cementitious materials' biggest drawbacks is their quasi-brittle nature and poor resistance to crack formation. Thus, many studies have been carried out to combine nano-fiber with cementitious composites to enhance their microstructure and mechanical properties, and results showed a small amount of carbon nanotubes (CNTs) can restrain the propagation of microcracks and improve the fracture toughness of the nanocomposites [1–3]. However, CNTs tend to agglomerate, hindering their dispersion in solvents because of their super high length-diameter ratio [4]. As a two-dimensional nanomaterial, graphene is the basic structural element of other allotropes, including graphite, CNTs and fullerenes [5,6]. The theoretical specific surface area (SSA) of graphene can reach 2630 m^2/g, which is much larger than that reported to date for CNTs [7]. In addition, it has an intrinsic tensile strength of 130 GPa and a Young's modulus of 1 TPa [8]. Due to its remarkable mechanical performance, great attention is paid to the graphene as the nano reinforcing material in cement with greatest potential.

Development of aqueous dispersions incorporating higher concentrations of graphene sheets would facilitate scalable production of graphene sheets modified concrete [9]. Thorough dispersion of graphene sheets in water is the key first step toward achieving uniform dispersions of graphene within cementitious composites [10]. Different surface treatments have been investigated for improving the hydrophilic property of graphene. Current processing methods involve acid treatment [2], oxidation via heating [11], ozone treatment [12] and silane treatment [13]. Because of graphene's innate attribute of hydrophobicity, oxidation treatment has been suggested as an effective method to achieve consistent yet durable

* Corresponding author at: College of Architecture and Civil Engineering, Zhejiang University of Technology, Hangzhou 310014, China.
E-mail address: yangyang@zjut.edu.cn (Y. Yang).

https://doi.org/10.1016/j.conbuildmat.2018.12.006
0950-0618/

aqueous dispersion [14], and these oxygen-containing functional groups attached to the graphene sheet improve its dispersion in water and cement matrix. Meanwhile, the bonding strength between graphene sheets and cement hydration products was also improved. Thus, many researchers have investigated the effects of graphene oxide (GO) on the mechanical properties of cement-based materials [15–18]. Lu et al. [19] demonstrated that the addition of GO shorted the setting time and decreased the workability of the magnesium potassium phosphate cement paste, but the mechanical properties of the composites were improved by GO. According to Chen [20], the compressive strengths of cement paste with 0.04 and 1 wt% GO are increased by 24.95% and 46.90%, respectively. Meng and Khayat [21] also indicated that the tensile strength of ultra-high-performance concrete was increased by 40% with the addition of 0.3% graphite nanoplatelets. Yang et al. [22] found that the hydrated degree of cement paste was increased with GO, but the C–S–H structure of the composite was not observed to have undergone any change. Li et al. [23] dispersed GO in a pore solution and cement paste, and GO dispersion in the cement paste was highly improved with the silica fume addition and 0.02 wt% GO was the appropriate amount. Lv et al. [24] reported that the introduction of 0.04% by weight of GO into cement paste produced a 37.5% improvement in the compressive strength at 28 days. Another study showed the same weight dose increased compressive strength by 14% [25]. In addition, an enhancement of about 41% has been achieved in tensile strength by incorporating 0.03 wt% GO sheets, and the hydration rate of cement can be accelerated by the nucleation effect of GO [26].

However, the process of oxidation lowering the mechanical properties of graphene sheets, and it exhibit a lower elastic modulus and tensile strength than graphene [27]. In the case of cementitious composites, there is still a need to develop a dispersion method for graphene sheets in water, and it should be low-cost and suitable for large-scale applications. Alkhateb et al. [28] compared the effects of pristine and acid-functionalized graphene on the microstructure and elastic modulus of cement paste, and results showed that the attachment of carboxyl (–COOH) and hydroxyl (–OH) groups increase the interfacial bond strength between graphene and C–S–H approximately 10 fold. Peyvandi et al. [10] investigated the flexural strength of cement with the addition of 0.13 wt% of graphite nanoplatelets, and various gains ranging from 27% to 73% were achieved. Sun et al. [29] observed that the compressive strength and elastic modulus of cement paste filled with multi-layer graphene increased by 54% and 50%, respectively. However, graphene would modestly weaken the compressive strength of cement by 20% under high addition due to the weak interfacial bonding strength between graphene and the cement matrix [30]. The main problem with using graphene is its negligible dispersibility in water, and avoiding entanglement and agglomeration of graphene is a perplexing challenge [14,31].

To achieve sufficient dispersion of graphene in cementitious materials, raw graphene sheets must be with enough dispersivity initially. In this work, with the supersonic and centrifuge as supplementary tools, the effects of surfactants on the dispersion of graphene in water were evaluated by ultraviolet–visible (UV–vis) absorption spectra and sedimentation test. Moreover, different amounts of added graphene sheets were considered (relative to the cement quantity): 0.01 wt%, 0.025 wt% and 0.05 wt%, and the influences of the graphene on the mechanical properties of the cement paste were investigated at different ages. Furthermore, scanning electron microscope (SEM), X-ray diffraction (XRD) and mercury intrusion porosimetry (MIP) were employed to investigate the degree of hydration and pore size distribution of graphene-cement composite, respectively.

2. Materials and methods

2.1. Materials

Ordinary Portland Cement P O 42.5 was used in this study and its chemical composition was given in Table 1. Graphene was purchased from Chengdu Organic Chemicals (China) Co. Ltd. and its properties were listed in Table 2. The morphology and particle diameter distribution of graphene sheets were shown in Fig. 1 and Fig. 2(a). The tributyl phosphate (TBP) provided by Aladdin Co. Ltd (Shanghai, China) was used to eliminate bubbles.

Different kinds of superficial active agents (SAAs) were used for graphene dispersion, including anionic surfactant sodium dodecyl benzene sulfonate ($C_{12}H_{25}C_6H_4SO_3Na$, AR), anionic surfactant sodium dodecyl sulfate ($CH_3(CH_2)_{11}SO_3Na$, AR), cationic surfactant CTAB ($C_{16}H_{33}(CH_3)_3NBr$, AR), and non-ionic surfactant Triton X-100 ($C_8H_{17}C_6H_4(OCH_2CH_2)_{10}OH$, AR). These SAAs were all purchased from Aladdin reagent (Shanghai, China) Co., Ltd. As a contrast, commercially available polycarboxylate superplasticizer (SP) from BASF was also used as an SAA to improve the workability.

2.2. Dispersion of graphene

Graphene tends to form aggregates due to strong intermolecular van der Waals interactions. Thus, the key to increasing the interfacial interaction between graphene and the cement matrix is improving the graphene dispersity. Recently, a variety of SAAs have been applied to solve the sedimentation problem of nanomaterials in aqueous solutions, such as sodium dodecyl sulfate (SDS), sodium dodecyl benzene sulfonate (SDBS), Triton X-100 (TX10), polycarboxylate superplasticizer, etc. In this study, the processes of ultrasonic dispersion and chemical functionalization were experimentally utilized to disperse graphene in aqueous solution. Thus, SDBS, SDS, TX10, CTAB and SP were initially chosen based on the literature. A probe type ultrasonic instrument of Scientz-750F model (20 kHz, 150–750 W, Ningbo, China) was used to disperse graphene sheets. The ultrasonic treatment equipment was designed for dispersing nanomaterials and it had the advantages of strong power output and good dispersion effect. The mechanical energy delivered by sonication was related to the sonication power. Thus, the study initially deals with the sonication power impacting on dispersion of graphene sheets, and the proper output power was selected and used for further study.

Furthermore, the TD 80-1 model centrifugal machine (Shanghai, China) with a maximum speed of 4000 rpm was employed to observe the stability of the graphene dispersion. The great surface area of graphene sheets means a high surface energy and agglomeration tendency, which needs an effective dispersion method. In this experiment, the mass ratios of graphene to SAAs were 1:2, 1:4, 1:6, and 1:8, and the entire dispersion procedure had the following steps:

(1) Firstly, the SAA was dissolved in water and stirred evenly. Then, graphene sheets were placed in this solution and stirred until the graphene were completely wetted, and this step took about 2 min.
(2) An ultrasonic disrupter (20 kHz, 450 W) was employed to disperse the graphene sheets in the solution. The sonication process was performed for 1–6 times, with a duration of each stage of 5 min. It was found that sonication caused both heating and foaming of the dispersion fluid. Therefore, the dispersion fluid was placed in ice water to de-foam after each sonication stage.

2.3. Preparation of specimens and testing procedure

The optimal ultrasonic dispersion time and graphene-to-surfactant mass ratios were determined by ultraviolet–visible (UV–vis) spectroscopy. According to the Beer–Lambert Law, the degree of dispersion of graphene sheets in water was evaluated using UV–vis spectroscopy, and the absorbance A can be measured as follow:

$$A = -log(I/I_0) = \varepsilon \cdot c \cdot d \quad (1)$$

Table 1
Chemical properties of cement (wt%).

Fe_2O_3	Al_2O_3	CaO	MgO	SiO_2	SO_3	Loss
2.91	4.58	61.08	3.19	19.50	2.50	3.60

Table 2
Properties of graphene sheets.

Purity	Thickness	Diameter	Specific surface area	Density	PH
99.5%	4–20 nm	2–16 μm	40 m^2/g	0.6 g/cm^3	7.3

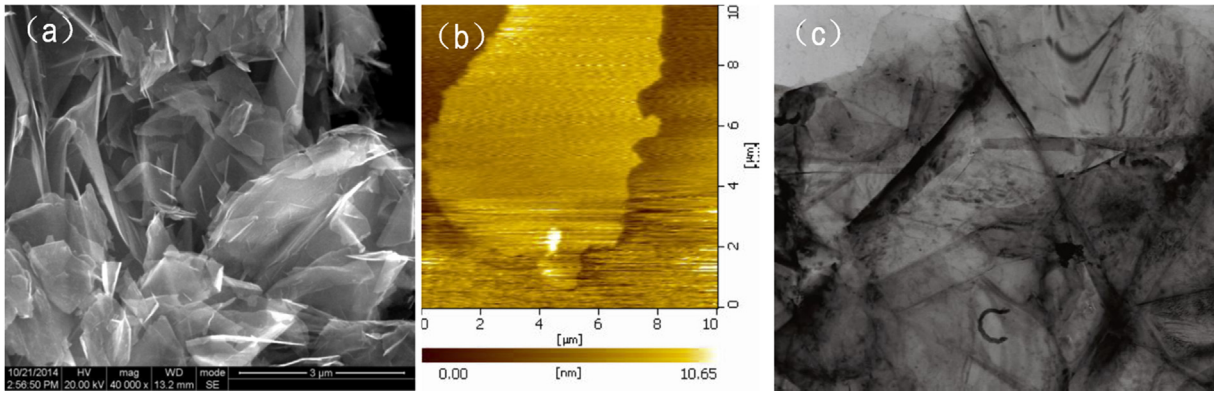

Fig. 1. Scanning electron microscope (a), atomic force microscope (b) and transmission electron microscope (c) images of graphene sheets.

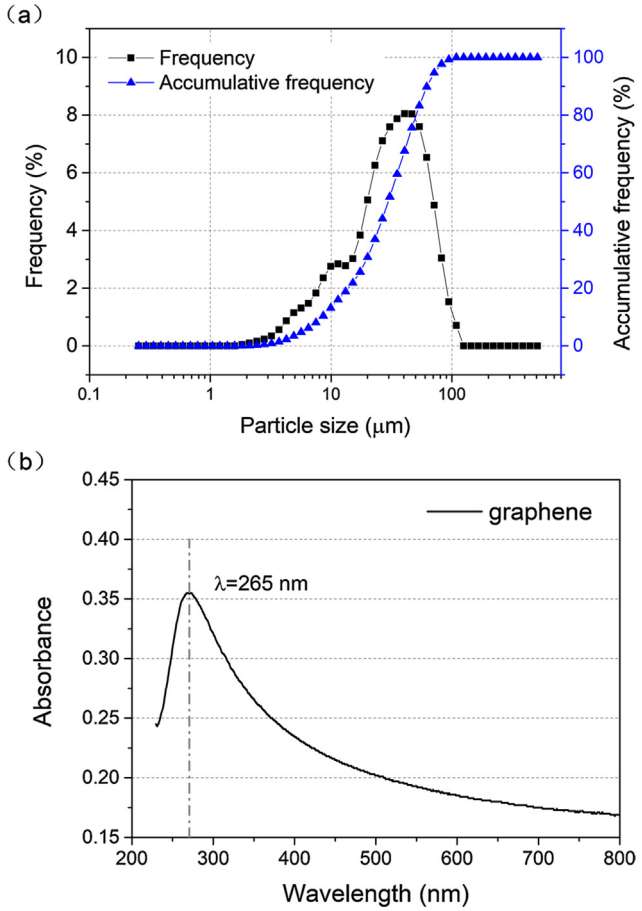

Fig. 2. The particle size distribution (a) and UV–vis spectrum (b) of graphene sheets.

where c and d are the concentration and the path length through the absorbing samples, respectively. For each species and wavelength, ε is a constant known as the molar absorptivity or extinction coefficient. The UV absorbance of graphene was shown in Fig. 2(b), and the absorbance maximum was around 265 nm.

Three different amounts of added graphene were considered (relative to the cement weight), in addition to a blank: 0.01 wt%, 0.025 wt% and 0.05 wt%. The mix proportion of all mixtures is shown in Table 3. The ratio of water to cement was 0.4 for all preparations, and it should be noted that the amount of water in the dispersion was also included. JJ-5 type cement mixer (Wuxi Jiangong Test Facility Co. Ltd., China) with the rotation rate 285 r/min was used for the mixing of cement paste, and the volume of the bowl was 5 L. The mixing process was as follows: firstly, graphene dispersion liquid and water were placed in the mixing pot and stirred for 60 s. Then, cement particles were placed into the pot and stirred for 180 s, and the cement paste appeared to be homogeneous. Finally, the paste was stirred at high-speed for another 120 s in order to effectively further disperse the graphene.

Table 3
Mix proportion of composite cement paste.

Type	Cement/g	SDBS/g	Graphene/g	TBP/g	Water/g
R1	100	0.06	0	0.2	40
G1	100	0.06	0.01	0.2	40
R2	100	0.15	0	0.2	40
G2	100	0.15	0.025	0.2	40
R3	100	0.3	0	0.2	40
G3	100	0.3	0.05	0.2	40

In accordance with Chinese standard GB/T 8077-2000 (Methods for testing uniformity of concrete admixture), the mixtures were poured into a truncated cone mold to perform the fluidity test immediately after mixing. The dimensions of the cone model were bottom diameter 60 mm, top diameter 36 mm, and height 60 mm. The cement paste was tipped into the mold and smoothed with a spatula. The mold was removed vertically, and the horizontal diameters of the paste were measured. After fluidity test, the cement paste was then poured into molds and vibrated for compaction.

According to Chinese standard GB/T1764-1999, cube specimens with dimensions of $40 \times 40 \times 40$ mm^3 were used for compression tests and samples with dimensions of $160 \times 40 \times 40$ mm^3 were prepared for flexural tests. Cubic compression and flexural strength were tested at the age of 3, 7 and 28 days, and the loading rate was set to 2.4 kN/s and 50 N/s, respectively. According to standard test ASTM C307-03, the tensile strength of cement paste containing different percentages of graphene sheets were investigated. The specimens were loaded in a tensile testing machine at a speed of 5 mm/min. The mechanical test was shown in Fig. 3. All samples were removed from their molds after 24 h and transferred to standard curing room (20 ± 2 °C, RH > 95%) for 28 days.

Furthermore, microstructure investigations were carried out with scanning electron microscope (SEM, FEI Quanta 650 FEG) and mercury intrusion porosimetry (MIP, AutoPore IV9500). Moreover, X-ray powder diffraction (XRD) data were test on a Bruker D8 Advance diffractometer.

3. Results and discussion

3.1. Effect of SAAs on the graphene dispersion

Due to the high specific surface area, graphene exists as large aggregates in water before ultrasonic treatment. During sonication, vibration produced by ultrasonic waves can overcome the van der Waals interactions between the graphene sheets and lead to their dispersion. The performances of surfactants CTAB, SDBS, SDS, TX100, and SP at various concentrations for graphene dispersion were tested. The absorption peak of graphene dispersion was measured at the wavelength of 265 nm for all spectra. The most suitable graphene/SAA weight ratio was estimated by comparing the absorbance of graphene dispersions containing the same amount of graphene and different amounts of surfactant. Furthermore,

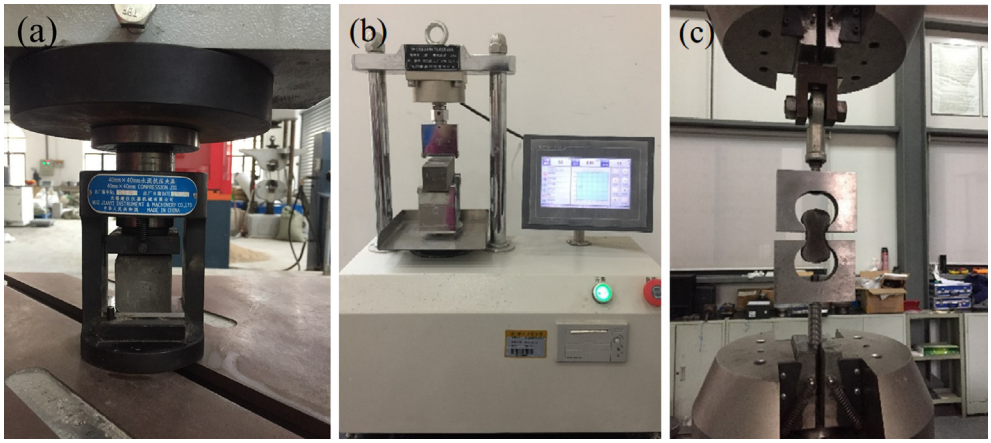

Fig. 3. Pictures of compressive (a), flexural (b) and tensile test (c) for specimens.

the UV–vis absorbency result of graphene solution without SAA was added as a reference sample.

Changing ultrasonic energy has a great effect on the dispersion degree of graphene, and more notably, the ultrasonic energy is related to the sonication power and time. Therefore, the influence of ultrasonic time and power on the absorbance of 0.05 wt% graphene dispersion was firstly analyzed. As shown in Fig. 4, the absorbance of graphene dispersion had higher values when output power was 450 W. In addition, the dispersion degree was optimized with 15 min of ultrasonic time.

For further study, the output power of 450 W was selected for ultrasonic dispersion process. Fig. 5(a) compares the evolution of the absorbance of 0.05 wt% graphene in aqueous solution for different optimum SAAs. It is advisable to plot the absorbance versus the total energy supplied to the dispersion instead of sonication time [32]. The general trends of the UV absorbance versus sonication time obtained for graphene–SDS and SDBS solutions were similar. The value of absorbance increases with sonication time and then reaches a saturation value, which corresponds to the maximum achievable degree of dispersion of the graphene in water. However, ultrasonic wave usually the rise of solution temperature, which cause the random molecular motion and decrease dispersion stability. Thus, prolonged sonication was negative to the dispersion degree of graphene.

Fig. 5(b) illustrates UV–vis spectra of graphene–SDBS solutions, obtained after different SDBS concentrations and sonication times. The addition of SDBS also accelerated the dispersion process, and the absorption peak remained stable after 15 min of sonication (corresponding to a total sonication energy of 270 kJ). It was found that the aqueous solution with high amount of SDBS exhibited higher dispersing capacity. A high level of SDBS produced an efficient coating on the surface of the graphene to prevent re-aggregation, however, an excessive dose of SDBS introduced a lot of bubbles. In this research, the optimum weight ratio of graphene to SDBS was identified as 1:6 by weight.

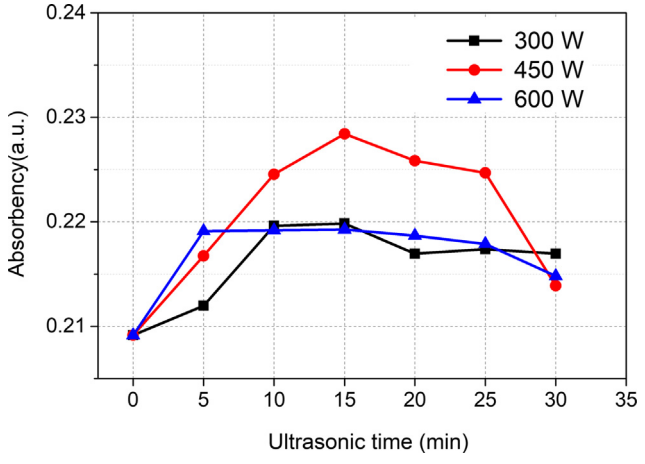

Fig. 4. Absorbance of graphene in aqueous solution with different sonication.

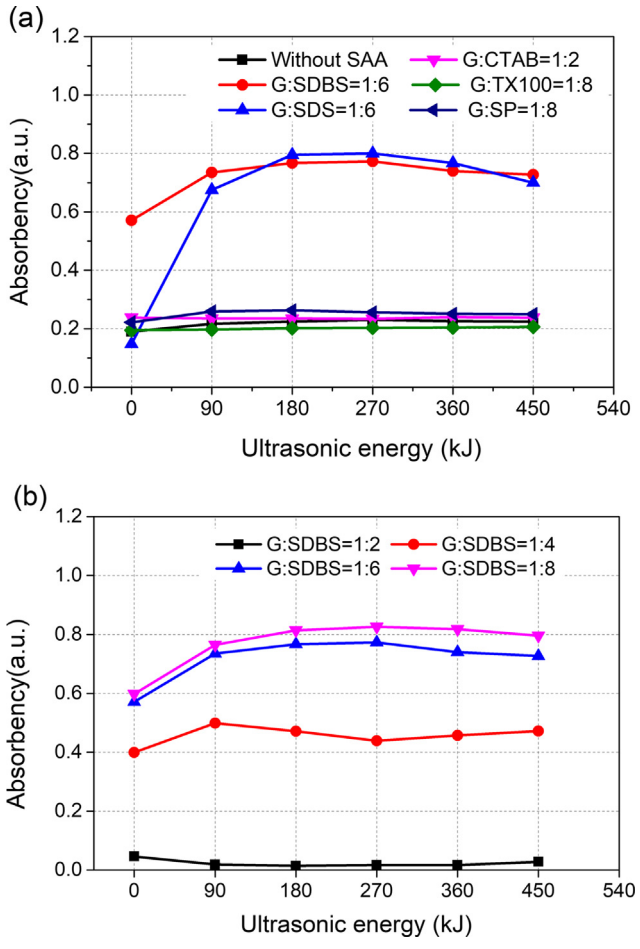

Fig. 5. UV–Vis spectrum of the graphene dispersion with different SAAs (a) and SDBS (b).

In this study, graphene sheets were used as raw materials and uniformly dispersion was obtained by using ultrasonication and surfactant treatment. However, there were still small amount of unexfoliated graphene sheets in the dispersion, and these graphene sheets would be hold together as clumps over time. Consequently, the poor dispersion of agglomerates in the matrix affect the strength of composites partly. Thus, most of previous studies used static settlement method to evaluate the long-term stability of dispersion. In this research, an acceleration sedimentation experiment was carried out using a centrifugal machine, which was usually employed for separating dense particles from solution. The agglomerates of graphene sheets were subjected to centrifugal force and sedimented at the bottom of the tube in a short time. The graphene solutions were put in a high-speed centrifuge for 20 min with a relative centrifugal force (RCF) of 1435*g*, which was equivalent to 20 days of natural precipitation. Firstly, graphene was dispersed with each type of surfactant with their optimal addition. Then, the mixture was centrifuged (2000 rpm, 20 min) to accelerate the stabilization stage. As previously mentioned, graphene was practically insoluble in water without physical or chemical modification. Graphene dispersion was treated by ultrasonic wave for 30 min without SAA, and sediment was observed at the bottom of the tube, as shown in Fig. 6. The graphene could maintain its well-dispersed state when SDBS was used as surfactants. The SDBS–graphene solutions remained totally opaque and homogeneous. Although the stability of solution with much longer time was not tested, the graphene sheets solution could maintain its well-dispersed state for a long time. Furthermore, we can improve the long-term stability of dispersion by reducing the concentration of graphene sheets and adding the centrifugal time.

The direct dispersion of hydrophobic graphene in water without the assistance of SAA has generally been considered to be a challenge. Fig. 5(b) showed the influence of different SDBS concentration on the absorbance of graphene in aqueous solution. The dispersion degree increased at the beginning of the sonication process. However, after 15 min of sonication (corresponding to a total sonication energy of 270 kJ), the value of absorbance reaches a plateau value, which corresponds to the maximum achievable degree of dispersion of the graphene in water. SDBS is a kind of anionic surfactants, which consist a hydrophilic sulfonate head-group and a hydrophobic alkylbenzene tail-group. The steric hindrance and electrostatic repulsion of SDBS were the main stabilizing dispersion mechanism. However, excessive SDBS concentration increased the number of like charges, which destroyed the balance force between graphene sheets and caused graphene particle to aggregate again [33,34]. Thus, over dosage surfactant had little promotion effect on the dispersion degree of graphene. Based on the graphene dispersion results determined by UV–vis spectroscopy, a graphene to-SDBS ratio of 1:6, and a sonication time of 15 min was used to prepare all dispersions used with cement paste.

3.2. Effect of graphene on fluidity of cement paste

The effects of graphene on fluidity of the cement paste were investigated using slump test, and the results are given in Fig. 7. Most of previous studies showed that the addition of graphene reduce workability of cementitious composites because of the high specific surface energy of graphene sheet. In this study, the influence of undispersed graphene on the fluidity of cement past was also tested. Three different amounts of added graphene were considered: 0.01 wt% (mix P1), 0.025 wt% (mix P2) and 0.05 wt% (mix P3), and SAA wasn't used and the ratio of water to cement was 0.4 for all preparations. Results showed that the fluidity of cement paste decreased with increasing addition of undispersed graphene sheets. Graphene was nearly 1000 times the specific surface area of

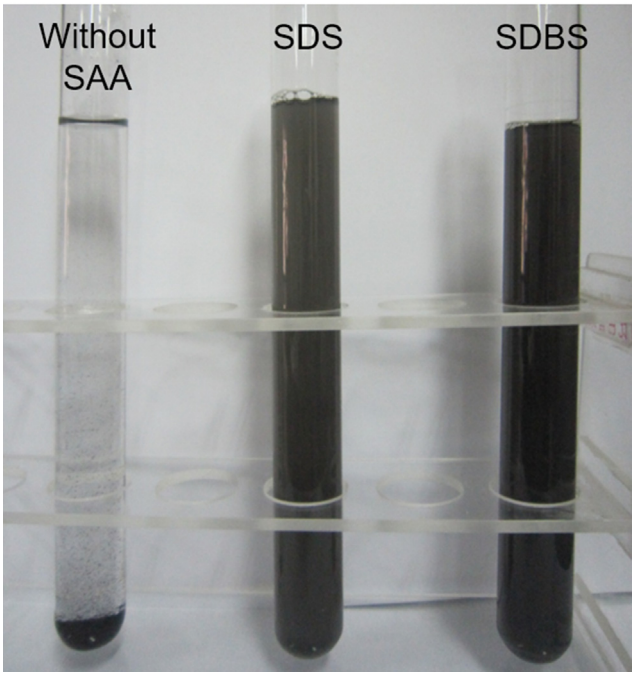

Fig. 6. Digital images of graphene dispersions after centrifugation.

cement particles, which increased the interaction between the cement particles and caused the degradation of cement paste liquidity.

At the same time, the impact of SDBS on the workability of cement paste was evaluated since the dosage of SDBS was 6 times of graphene. Fig. 7 indicated that the increased content of SDBS had an adverse effect on the fluidity of cement paste, especially when the amount of SDBS was high. SDBS used in this research was a type of anionic surfactants with amphiphilic structures, and its steric hindrance and electrostatic repulsion were the main stabilizing dispersion mechanism. Considering the dosage of SDBS was 6 times of that of graphene sheets, SDBS could have an impact on the workability of cement paste. Test results in Fig. 7 also suggested that the influence of additives on workability was stronger for SDBS than for graphene sheets, and the increased content of SDBS had an adverse effect on the fluidity of cement paste. Compared with P1 and R1 group, the low adding amount of SDBS slightly improved the workability of cement paste, which is

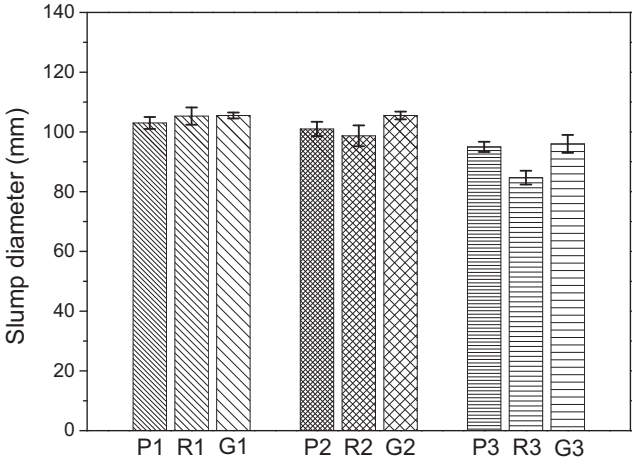

Fig. 7. Slump test results of mixtures.

consistent to reported literature. When SDBS concentrations reach the critical micellar level in aqueous solution, the surface tension of the solution was increased, and the stability of dispersion was reduced [35]. It explained why the workability of R3 was reduced significantly when the amount of SDBS was high, as shown in Fig. 7.

It was found that the workability of the G2 and G3 group was higher than their control groups (R2 and R3). There existed a strong bonding interaction between the benzene ring of the SDBS and graphene due to the π-π stacking interactions [36]. During the dispersion process, the co-action of electrostatic repulsion and steric hindrance of SDBS decreased graphene surface energy, which improved the dispersing performance of solution [37]. In this case, excess SDBS adsorb on the surface of graphene sheets when graphene sheets was added into the solution. Therefore, the addition of graphene mitigated the impact of high dosage SDBS on the workability of paste, and the fluidity of G2 and G3 mixture were improved.

3.3. Compressive and flexural strengths

The influence of different amount of graphene on the mechanical properties of cement paste was investigated, and the test results are presented in Fig. 8. For the compressive and bending tests, the standard deviation of the six specimens was lower than 10%, which indicated that the dispersion process was effective for dispersing graphene in a cementitious matrix. Fig. 8(a) shows the compressive strength of specimens at 3, 7 and 28 days. With the addition of 0.01 wt% and 0.025 wt% graphene sheets, the compressive strength of cement paste was enhanced (relative to their control group). Compared with the R2 group, the compressive strengths of the G2 group were increased by 23.7%, 14.9% and 10.0% at 3, 7 and 28 days, respectively. Similarly, the compressive strengths of the G1 group were increased by 15%, 5.1% and 13.5% at 3, 7 and 28 days, respectively. However, a high amount of graphene sheets (0.05 wt%) led to a decrease in the compressive strength of the cement paste; this was for the following reasons: firstly, the use of SDBS caused the formation of foam and increased the porosity of the matrix; secondly, increasing the graphene sheets concentration may result in an increased number of graphene agglomerates, which reduced the interfacial bond between graphene sheets and cement hydration.

The incorporation of well-dispersed graphene also increased the flexural strength of cement paste beams, as shown in Fig. 8 (b). The addition of 0.01 wt% graphene produced a slight increase in the flexural strength at different ages. Compare to the R2 sample, the flexural strengths of specimens containing 0.025 wt% graphene were improved by 12.5%, 23.6%, and 16% at 3, 7 and 28 days, respectively. The flexural strength of cement paste was primarily affected by the presence of macro-defects that were inevitably introduced during the mixing process. As an ideal two-dimensional nano-material, graphene may improve the cement matrix resistance to cracking by offsetting the coalescence of smaller cracks into larger micro-cracks. However, the flexural strength of the G3 group was significantly decreased with the addition of 0.05 wt% graphene sheets, which was similar to the situation of compressive strength.

3.4. Tensile strength

The results of tensile strength tests of each group at 3, 7, and 28 days are shown in Fig. 9. The tensile strength of the specimens increased with increasing curing age. The addition of graphene sheets had obvious influence on the tensile strength of samples at an early age. Compared with their control groups, the 3-day tensile strength of samples containing 0.01 wt% and 0.025 wt% graphene sheets increased 18.6% and 16.7%, respectively. At 7 days, the tensile strength of G1 and G2 increased by 14.1% and 15.2% respectively, compared with R1 and R2. However, continued increase of graphene sheets could not improve the strength of the cement paste; the tensile strength of specimens containing 0.05 wt% graphene sheets was almost same as the control group at different curing ages. This may be attributed to the agglomeration of the graphene sheets in the cement matrix. It was difficult to achieve uniform distribution of graphene sheets throughout the matrix, and graphene sheets can more easily aggregate with the increase of volume fraction. Agglomeration of graphene sheets hindered their potential to improve the mechanical properties of cement-based materials.

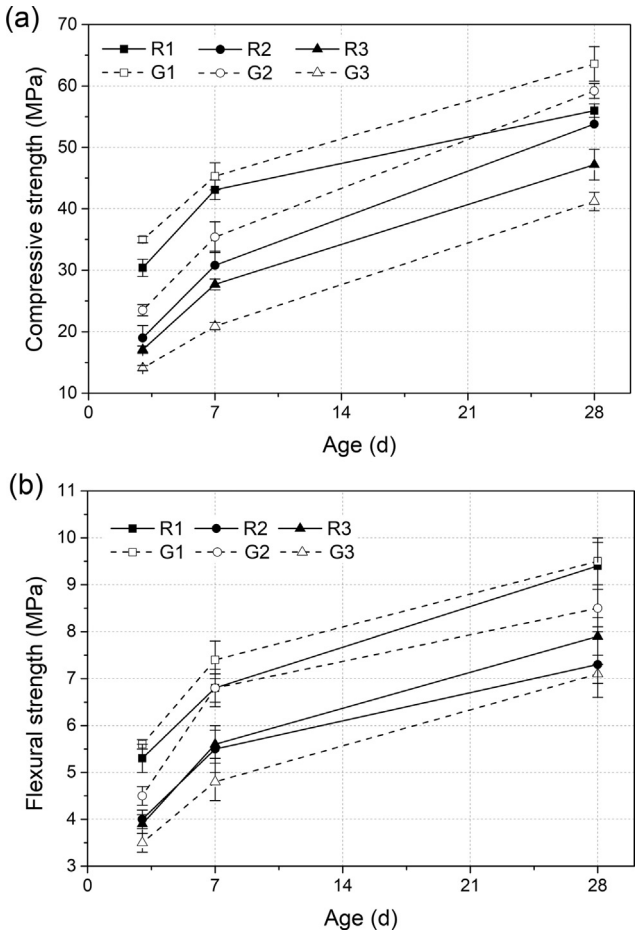

Fig. 8. Compressive and flexural strengths of samples at 3, 7 and 28 days.

3.5. Morphology and microstructure

The microstructural characteristics of cement paste affect its mechanical properties. The cement hydration products were compacted at 28 days, and graphene sheets could barely be distinguished. Thus, the distribution and condition of graphene sheets in the cement paste were observed at 7 days. Fig. 10(a) shows the microstructure images of cement paste without graphene sheets. The structure of products is loose and there are many defects in them. Considering that the micrographs of hexagonal platy crystals of calcium hydroxide (CH) are similar to that of graphene, the EDS analysis result was employed to determine the existence of graphene sheets. The areas with box markings in Fig. 10 are the selected areas for EDS detection, and the results are shown in Table 4. It can be found that area II, III and Ⅳ contain

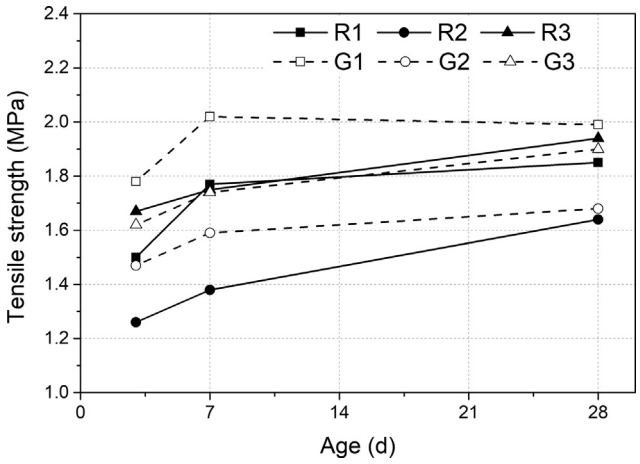

Fig. 9. Tensile strength of samples at 3, 7 and 28 days.

a lot of calcium, silicon and oxygen elements, it may be due to the active functional groups on the surface of graphene sheets promote the formation of hydrated products.

For the G1 and G2 groups at 7 days (Fig. 10(b) and (c)), graphene sheets were mostly found as individual sheet with a particle size of below 5 μm indicating that an effective dispersion was achieved. Moreover, graphene sheets had a seeding effect in the cement hydration, which advanced the growth of hydration products. As indicated in Fig. 10(c), graphene was mostly found as individual graphene sheet, thus showing that a good dispersion was achieved by means of SDBS and sonication. In addition, graphene was coated by cement hydrates in the majority of the areas inspected. As shown in Fig. 10(d), a crack-bridging mechanism of well-bonded graphene sheets in cement matrix at 0.025 wt% inhibited crack development. Graphene sheets formed a net-like arrangement showing good incorporation into the cement matrix, as Fig. 10(e) shows.

The typical microstructure of graphene-reinforced cement paste at 0.05 wt% concentration was illustrated in Fig. 10(f), and agglomerates were found more frequently on the fracture surfaces of samples. Obvious voids can be seen in the interfacial zone between graphene sheets and the cement hydration products. High levels of graphene weakened the strength of cement, which can be attributed to defects resulting from a less effective compaction. In addition, the poor dispersion of graphene in the matrix and the low fluidity of the paste also decreased the strength of composites and the natural morphology of graphene with a wrinkled structure could be identified. However, wrinkles in graphene may improve the interlocking mechanism, which has a positive effect on the mechanical properties of the matrix [38].

3.6. XRD analysis

The XRD patterns of the cement paste modified with different graphene sheets additions are shown in Fig. 11. Portlandite (CH), ettringite (AFt), tricalcium silicate (C_3S) and dicalcium silicate (C_2S) were found to be major phases for samples. Moreover, the amount of these hydration products increases with increasing hydration time. The XRD results showed the amount of calcium silicate hydrates (C–S–H) gels in G1 and G2 samples was higher than in the normal cement paste (R1 and R2), which was caused by the nucleation of C–S–H by the graphene sheets.

The orientation index reflect the growth of CH crystal during cement hydration, and the influence of graphene sheets on CH orientation can be determined by XRD pattern [39]. In general, the lower orientation index, the more compact of hardening cement paste [40,41]. The orientation index in part reflect the mechanical strength enhancement of graphene. According to Grandet and Ollivier [42], the (1 0 1) crystal plane of CH could be used as a reference plane, and the orientation index R of (0 0 1) crystal plane can be calculated by $R = 1.35 \times I_{(0\,0\,1)}/I_{(1\,0\,1)}$, where $I_{(0\,0\,1)}$ and $I_{(1\,0\,1)}$ are (0 0 1) and (1 0 1) crystal face peak intensity of CH crystal, respectively. As shown in Fig. 11(d), orientation indexes of the

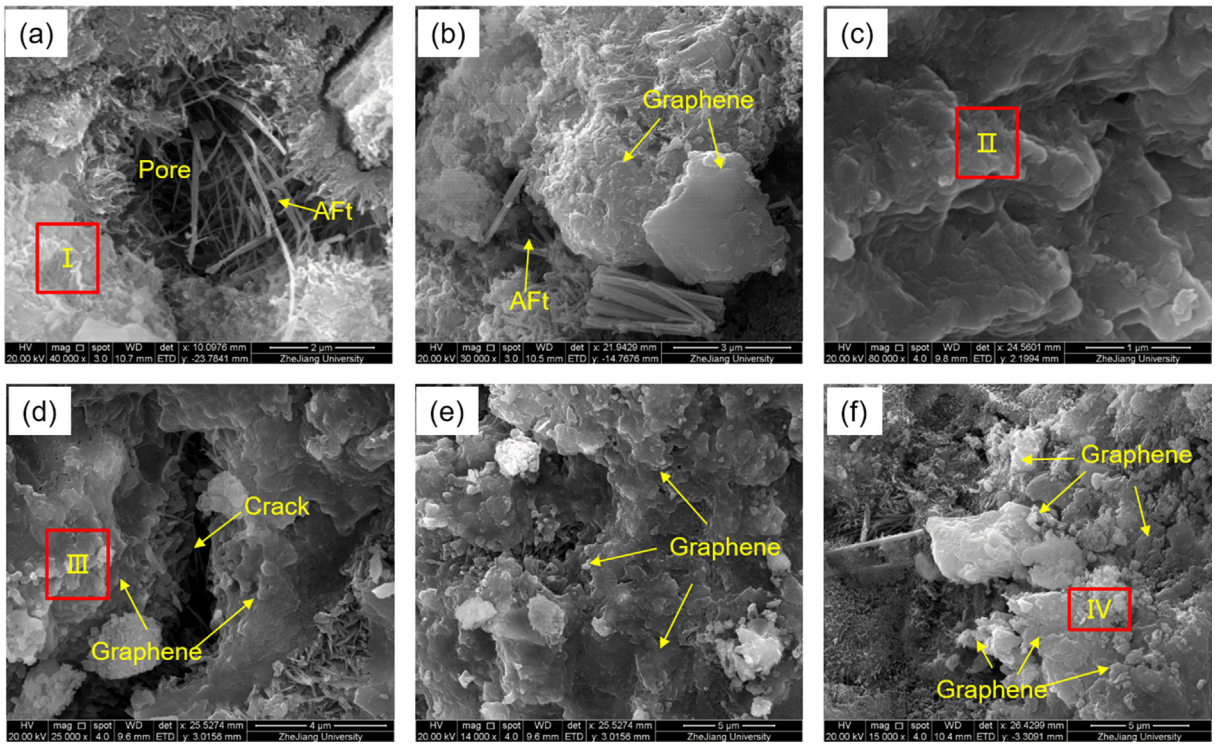

Fig. 10. SEM micrographs of the R1 (a), G1 (b), G2 (c, d, e) and G3 (f) samples at 7 days.

Table 4
EDS test results.

Area	Element (wt%)					
	Ca	O	Si	Al	Mg	C
Ⅰ	72.9	18.3	5.3	1.5	1.6	0.4
Ⅱ	50.2	33.0	9.6	1.8	0.8	4.6
Ⅲ	48.9	33.2	11.5	1.3	0.4	4.7
Ⅳ	41.1	38.0	10.2	3.0	1.5	6.2

R2 sample were 2.6, 1.88 and 1.63 at ages of 3d, 7d and 28d, respectively, and the indexes of the G2 sample were 1.87, 1.71 and 1.43. The addition of 0.025 wt% graphene sheets lowered the orientation index of CH crystals significantly, which enhances the interface properties of cement-based materials.

3.7. Porosity and pore size distribution

By using MIP analysis, the pore information of cement paste with different amounts of graphene sheets at 7 days is summarized in Table 5. The experimental results indicated that a high concentration of SDBS leads to foam formation and high porosity of the cement paste. However, the results also verified that the pores in cement paste were refined through the addition of graphene sheets. Compared with the R2 group, the total porosity of samples decreases from 29.580% to 28.739% by incorporating 0.025 wt% of graphene sheets. Meanwhile, the median pore diameter and average pore diameter of the G2 group were also reduced. These indicated that the addition of graphene sheets increased the compactness of the matrix. Consequently, the strength of the cement paste was increased by the addition of graphene sheets due to the improved pore characterization. Although the total porosity of the G3 sample was higher than that of R3, the average pore diameter of the cement was reduced from 41.2 nm to 34.1 nm with the addition of 0.05 wt% of graphene sheets. The relationship between the log differential intrusion and pore size diameter is shown in Fig. 12. It demonstrated that the addition of 0.025 wt% and 0.01 wt% of graphene sheets refined the microstructure of cement paste by reducing the number of macroscopic pores (>50 nm).

4. Discussion

The main challenges associated with the incorporation of graphene are attaining uniform dispersion and interfacial bonding within the cement matrix. The dispersion process is shown in Fig. 13; the ultrasonication formed a cavitation field and produced millions of microbubbles during the dispersion, which accelerated the exfoliation of graphene agglomerates. However, excessive sonication may result in breakage of graphene sheets, reducing their aspect ratio. The proper choice of a suitable surfactant and sonication time require consideration of its structure and its optimum ratio to graphene. Previous studies have shown that anionic surfactants have higher dispersion capability than cationic surfactants or

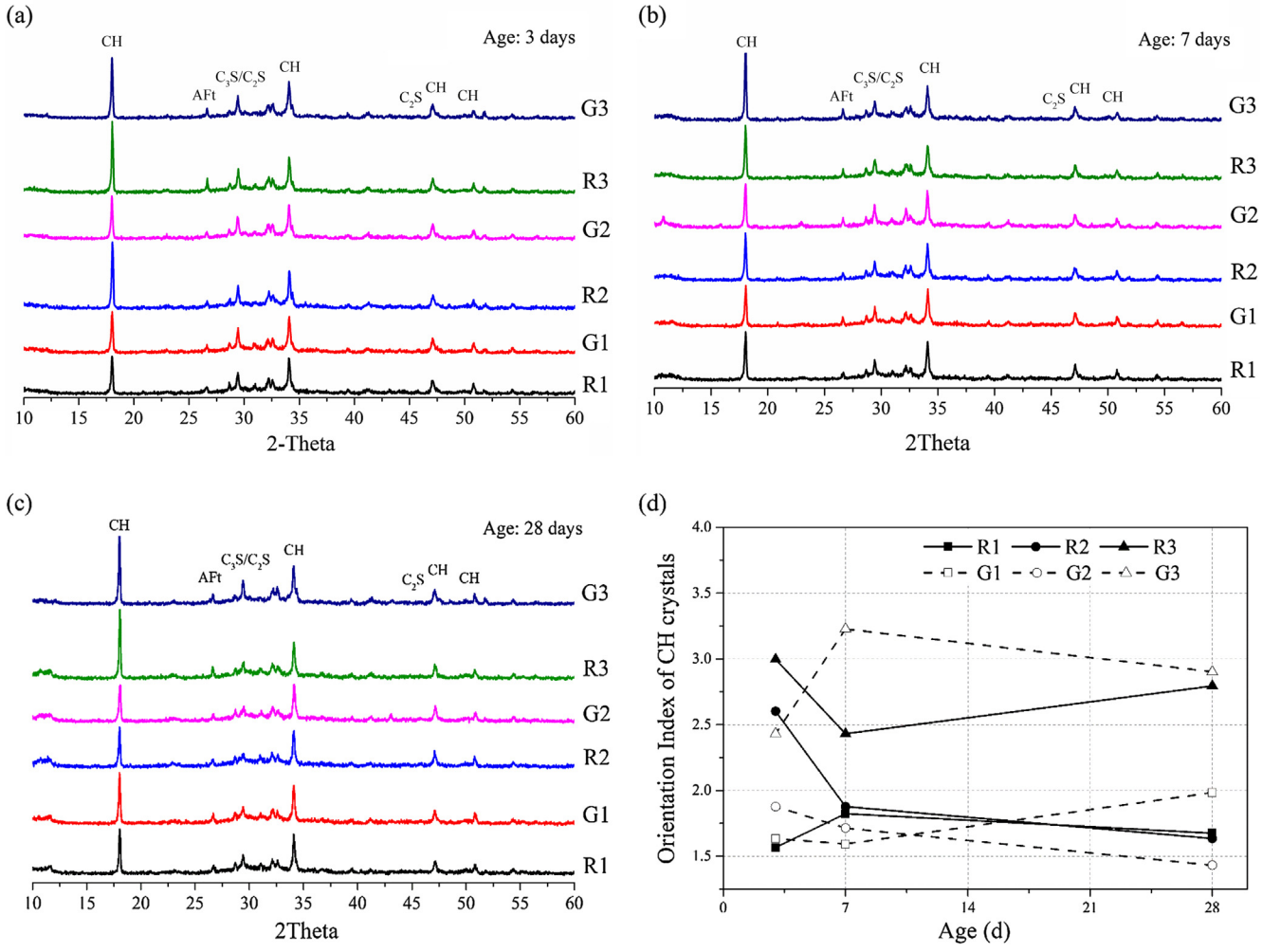

Fig. 11. XRD analysis of composites at 3 (a), 7 (b) and 28 (c) days, and orientation index of CH crystals (d).

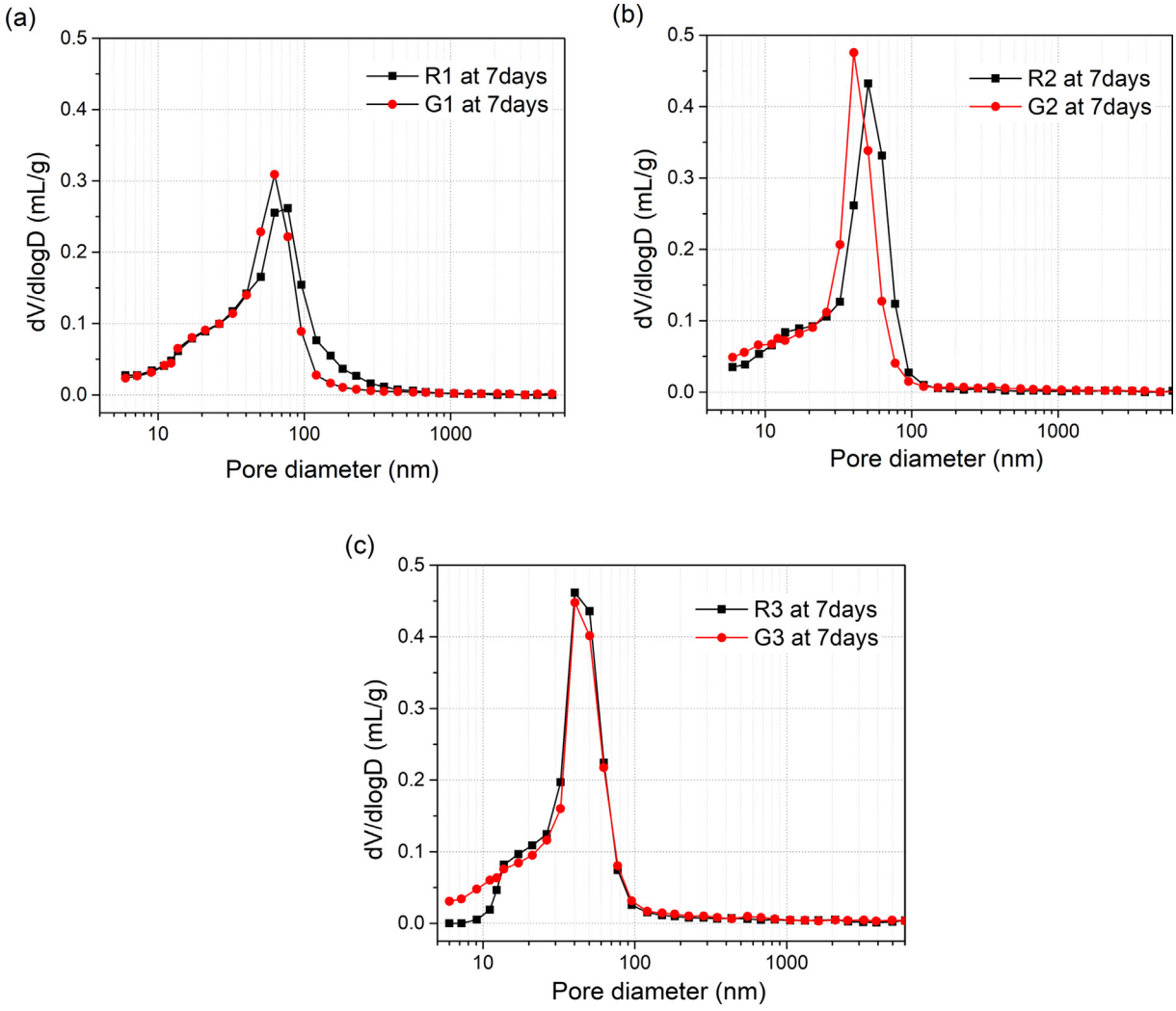

Fig. 12. Pore size distribution of samples at 7 days.

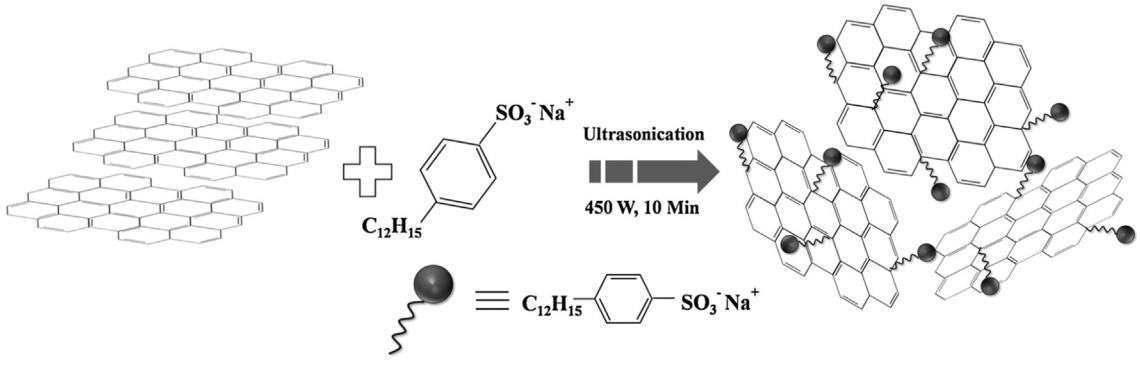

Fig. 13. Schematic representations of the mechanisms by SDBS help disperse graphene.

Table 5
MIP analysis of specimens at 7 days.

No.	Total intrusion volume (mL/g)	Porosity (%)	Median pore diameter (nm)	Average pore diameter (nm)
R1	0.1695	27.151	63.8	37.9
G1	0.1591	26.472	58.2	36.2
R2	0.1861	29.580	51.3	32.5
G2	0.1818	28.739	43.7	29.0
R3	0.1953	30.279	48.5	41.2
G3	0.1997	31.137	48.1	34.7

nonionic surfactants [43]. In this study, the dispersing performance of these five surfactants followed a decreasing sequence of SDBS > SDS > SP > CTAB > TX100, and graphene with a mixing ratio of 1:6 by weight of SDBS exhibited the best dispersion performance. Although higher surfactant concentration was helpful in improving the suspension homogeneity of graphene, excessive addition of surfactant might have negative effects on graphene reinforced cement-based materials. The oxygenated groups on the surface of graphene lead to hydrophilicity of the graphene, and improve interfacial bonding strength between graphene and cement paste.

This study also indicated that the reinforcing effects of graphene sheets on cement were realized through a filling effect, crack bridging and the regulation of the cement hydration products. The incorporation of graphene sheets reduced the porosity of the cement paste and resulted in a more compact structure. The mechanical test results showed that the graphene sheets improve the strength of the cement paste, especially at an early age. Compared to conventional fibers, graphene, in terms of its superior aspect ratio, has a seeding effect on the cement hydration kinetics, stimulating the growth of hydration products. Furthermore, the interfacial adhesion by graphene's functional groups improved the covalent bonds between graphene and hydration products, which makes graphene sheets a promising material for hindering microcrack propagation.

5. Conclusions

The influence of SAAs on the stability and dispersion of graphene in water was investigated using sonication and UV–Vis spectroscopy. SDBS was considered as the most effective dispersant of all the SAAs, followed by SDS, SP, CTAB and TX100. Moreover, a graphene-to-SDBS ratio of 1:6 led to the uniform dispersion of graphene sheets in aqueous solution.

Increases in compressive, flexural and tensile strengths were observed for all mixtures prepared with the addition of 0.025 wt % of graphene, reaching improvements up to 14.9%, 23.6% and 15.2% at 7 days, respectively. However, increasing the graphene concentration to 0.05 wt% resulted in reduced strengths in cement, because the agglomeration behavior of graphene sheets limits the reinforcing effect on cementitious materials.

Microscopic examination of the specimens showed the graphene promoted the hydration reaction of cement and acted as a discontinuous network or as an individual sheet. It was revealed that graphene improved the binding of neighboring C–S–H clusters and bridged the voids between them. MIP test results indicated that graphene sheets refined the pore structure and reduced the total porosity of the cement paste, making the matrix much more compact. Moreover, the orientation index of CH crystals was decreased by the addition of graphene.

Conflict of interest

The authors declare that there are no known conflicts of interest associated with this publication and there has been no significant financial support for this work that could have influenced its outcome.

Acknowledgement

The authors would like to acknowledge the financial supports provided by the National Natural Science Foundation of China (No. 51708501 and No. 51778583).

References

[1] S. Xu, J. Liu, Q. Li, Mechanical properties and microstructure of multi-walled carbon nanotube-reinforced cement paste, Constr. Build. Mater. 76 (2015) 16–23.
[2] G.Y. Li, P.M. Wang, X. Zhao, Mechanical behavior and microstructure of cement composites incorporating surface-treated multi-walled carbon nanotubes, Carbon 43 (6) (2005) 1239–1245.
[3] M.S. Konsta-Gdoutos, Z.S. Metaxa, S.P. Shah, Highly dispersed carbon nanotube reinforced cement based materials, Cem. Concr. Res. 40 (7) (2010) 1052–1059.
[4] A. Cwirzen, K. Habermehl-Cwirzen, V. Penttala, Surface decoration of carbon nanotubes and mechanical properties of cement/carbon nanotube composites, Adv. Cem. Res. 20 (2) (2008) 65–74.
[5] K.S. Novoselov, A.K. Geim, S.V. Morozov, D. Jiang, M.I. Katsnelson, I.V. Grigorieva, et al., Two-dimensional gas of massless dirac fermions in graphene, Nature 438 (7065) (2005) 197–200.
[6] A.K. Geim, K.S. Novoselov, The rise of graphene, Nat. Mater. 6 (3) (2007) 183–191.
[7] F. Bonaccorso, L. Colombo, G. Yu, M. Stoller, V. Tozzini, A.C. Ferrari, et al., Graphene, related two-dimensional crystals, and hybrid systems for energy conversion and storage, Science 347 (6217) (2015) 1246501.
[8] C. Lee, X. Wei, J.W. Kysar, J. Hone, Measurement of the elastic properties and intrinsic strength of monolayer graphene, Science 321 (5887) (2008) 385–388.
[9] A. Yazdanbakhsh, Z. Grasley, B. Tyson, R.A. Al-Rub, Challenges and benefits of utilizing carbon nanofilaments in cementitious materials, J. Nanomater. 3 (2012) 4661–4677.
[10] A. Peyvandi, P. Soroushian, N. Abdol, A.M. Balachandra, Surface-modified graphite nanomaterials for improved reinforcement efficiency in cementitious paste, Carbon 63 (2) (2013) 175–186.
[11] J.J. George, A.K. Bhowmick, Fabrication and properties of ethylene vinyl acetate-carbon nanofiber nanocomposites, Nanoscale Res. Lett. 3 (12) (2008) 508–515.
[12] N. Leconte, J. Moser, P. Ordejón, H. Tao, A. Lherbier, A. Bachtold, et al., Damaging graphene with ozone treatment: a chemically tunable metal-insulator transition, ACS Nano 4 (7) (2010) 4033–4038.
[13] Y.J. Wan, L.X. Gong, L.C. Tang, L.B. Wu, J.X. Jiang, Mechanical properties of epoxy composites filled with silane-functionalized graphene oxide, Compos. Part A 64 (64) (2014) 79–89.
[14] A.H. Korayem, N. Tourani, M. Zakertabrizi, A.M. Sabziparvar, W.H. Duan, A review of dispersion of nanoparticles in cementitious matrices: nanoparticle geometry perspective, Constr. Build. Mater. 153 (2017) 346–357.
[15] K. Gong, Z. Pan, A.H. Korayem, L. Qiu, D. Li, F. Collins, et al., Reinforcing effects of graphene oxide on portland cement paste, J. Mater. Civ. Eng. 27 (2) (2015) A4014010.
[16] I. Rhee, Y.A. Kim, G. Shin, J.H. Kim, H. Muramatsu, Compressive strength sensitivity of cement mortar using rice husk-derived graphene with a high specific surface area, Constr. Build. Mater. 96 (2015) 189–197.
[17] S. Chuah, Z. Pan, J.G. Sanjayan, C.M. Wang, W.H. Duan, Nano reinforced cement and concrete composites and new perspective from graphene oxide, Constr. Build. Mater. 73 (2014) 113–124.
[18] Z. Lu, A. Ahanif, G. Sun, R. Liang, P. Parthasarathy, Z. Li, Highly dispersed graphene oxide electrodeposited carbon fiber reinforced cement-based materials with enhanced mechanical properties, Cem. Concr. Comp. (2018).
[19] Z. Lu, D. Hou, H. Ma, T. Fan, Z. Li, Effects of graphene oxide on the properties and microstructures of the magnesium potassium phosphate cement paste, Constr. Build. Mater. 119 (2016) 107–112.
[20] Z. Chen, X. Zhou, X. Wang, P. Guo, Mechanical behavior of multilayer go carbon-fiber cement composites, Constr. Build. Mater. 159 (2018) 205–212.
[21] W. Meng, K.H. Khayat, Mechanical properties of ultra-high-performance concrete enhanced with graphite nanoplatelets and carbon nanofibers, Compos. B Eng. 107 (2016) 113–122.
[22] H. Yang, M. Monasterio, H. Cui, N. Han, Experimental study of the effects of graphene oxide on microstructure and properties of cement paste composite, Compos. A Appl. Sci. Manuf. 102 (2017) 263–272.
[23] X. Li, A.H. Korayem, C. Li, Y. Liu, H. He, J.G. Sanjayan, et al., Incorporation of graphene oxide and silica fume into cement paste: a study of dispersion and compressive strength, Constr. Build. Mater. 123 (2016) 327–335.
[24] S. Lv, Y. Ma, C. Qiu, T. Sun, J. Liu, Effect of graphene oxide nanosheets of microstructure and mechanical properties of cement composites, Constr. Build. Mater. (2013).
[25] X. Li, Y.M. Liu, W.G. Li, C.Y. Li, J.G. Sanjayan, W.H. Duan, et al., Effects of graphene oxide agglomerates on workability, hydration, microstructure and compressive strength of cement paste, Constr. Build. Mater. 145 (2017).
[26] M.M. Mokhtar, S.A. Abo-El-Enein, M.Y. Hassaan, M.S. Morsy, M.H. Khalil, Mechanical performance, pore structure and micro-structural characteristics of graphene oxide nano platelets reinforced cement, Constr. Build. Mater. 138 (2017) 333–339.
[27] D.G. Papageorgiou, I.A. Kinloch, R.J. Young, Graphene/elastomer nanocomposites, Carbon 95 (2015) 460–484.
[28] H. Alkhateb, A. Al-Ostaz, A.H. Cheng, X. Li, Materials genome for graphene-cement nanocomposites, J. Nanomech. Micromech. 3 (3) (2013) 67–77.
[29] S. Sun, S. Ding, B. Han, S. Dong, X. Yu, D. Zhou, et al., Multi-layer graphene-engineered cementitious composites with multifunctionality/intelligence, Compos. B Eng. 129 (2017) 221–232.

[30] J. Xu, D. Zhang, Pressure-sensitive properties of emulsion modified graphene nanoplatelets/cement composites, Cem. Concr. Compos. 84 (2017) 74–82.
[31] L. Rodriguez-Perez, M.Á. Herranz, N. Martín, The chemistry of pristine graphene, Chem. Commun. 49 (36) (2013) 3721–3735.
[32] J. Yu, N. Grossiord, C.E. Koning, J. Loos, Controlling the dispersion of multi-wall carbon nanotubes in aqueous surfactant solution, Carbon 45 (3) (2007) 618–623.
[33] Z. Sun, V. Nicolosi, D. Rickard, S.D. Bergin, D. Aherne, J.N. Coleman, Quantitative evaluation of surfactant-stabilized single-walled carbon nanotubes: dispersion quality and its correlation with zeta potential, J. Phys. Chem. C 112 (29) (2008) 10692–10699.
[34] K. Yurekli, C.A. Mitchell, R. Krishnamoorti, Small-angle neutron scattering from surfactant-assisted aqueous dispersions of carbon nanotubes, J. Am. Chem. Soc. 126 (32) (2004) 9902–9903.
[35] L. Vaisman, H.D. Wagner, G. Marom, The role of surfactants in dispersion of carbon nanotubes, Adv. Colloid Interfac. 128 (2006) 37–46.
[36] M. Bystrzejewski, A. Huczko, H. Lange, T. Gemming, B. Büchner, M.H. Rümmeli, Dispersion and diameter separation of multi-wall carbon nanotubes in aqueous solutions, J. Colloid Interface Sci. 345 (2) (2010) 138–142.
[37] C.C. West, J.H. Harwell, Surfactants and subsurface remediation, Environ. Sci. Technol. 26 (12) (1992) 2324–2330.
[38] D. Galpaya, M. Wang, C. Yan, M. Liu, N. Motta, E. Waclawik, Fabrication and mechanical and thermal behaviour of graphene oxide/epoxy nanocomposites, Livest Sci. 151 (2–3) (2013) 152–157.
[39] B. Han, Q. Zheng, S. Sun, S. Dong, L. Zhang, X. Yu, et al., Enhancing mechanisms of multi-layer graphenes to cementitious composites, Compos. A Appl. Sci. Manuf. 101 (2017) 143–150.
[40] T. Meng, Y. Yu, X. Qian, S. Zhan, K. Qian, Effect of nano-tio 2 on the mechanical properties of cement mortar, Constr. Build. Mater. 29 (3) (2012) 241–245.
[41] Q. Ye, Z. Zhang, D. Kong, R. Chen, Influence of nano-sio addition on properties of hardened cement paste as compared with silica fume, Constr. Build. Mater. 21 (3) (2007) 539–545.
[42] J. Grandet, J.P. Ollivier, Etude de la formation du monocarboaluminate de calcium hydrate au contact d'un granulat calcaire dans une pate de ciment portland, Cem. Concr. Res. 10 (6) (1980) 759–770.
[43] J. Luo, Z. Duan, H. Li, The influence of surfactants on the processing of multi-walled carbon nanotubes in reinforced cement matrix composites, Phys. Status Solidi (a) (2009) 2783–2790.